FLUME STUDY ON DRIFTWOOD CAPTURING SYSTEM USING RECTANGULAR EMBAYMENT ZONE

TAKAAKI OKAMOTO
Department of Civil Engineering, Kyoto University, Kyoto 615-8540, Japan, e-mail okamoto.takaaki.8x@kyoto-u.ac.jp

MICHIO SANJOU
Department of Civil Engineering, Kyoto University, Kyoto 615-8540, Japan, e-mail michio.sanjou@water.kuciv.kyoto-u.ac.jp

ABSTRACT

At the time of localized torrential rains, wood on a mountain surface is washed onto rivers and these driftwood in rivers aggravate the flood events. For example, large driftwood accumulates at a bridge and blocks a river, which lead to flooding of the nearby areas. In the present study, we considered the driftwood capturing structure using an embayment zone to remove woody debris from the river. The laboratory flume experiments were conducted and we investigated the trapping probability of driftwood in the embayment zone. To induce the model logs toward the embayment zone, the groyne is installed on the opposite side of the embayment zone. The results indicated that the trapping probability is highly influenced by the groyne position and the goyne length. When Groyne2 was installed upstream of Groyne1, woody debris can be trapped in the embayment zone efficiently without using long groyne.

Keywords: Driftwood capturing structure; embayment zone; PIV

1. INTRODUCTION

Climate change increases the frequency of natural disasters such as torrential rains and floods. At the time of localized torrential rains, wood on a mountain surface is washed onto rivers and these driftwood in rivers aggravate the flood events (Fig.1, Okamoto et al. 2016). For example, large driftwood accumulates at bridge and blocks the river, which lead to increased water levels and flooding of the nearby areas.

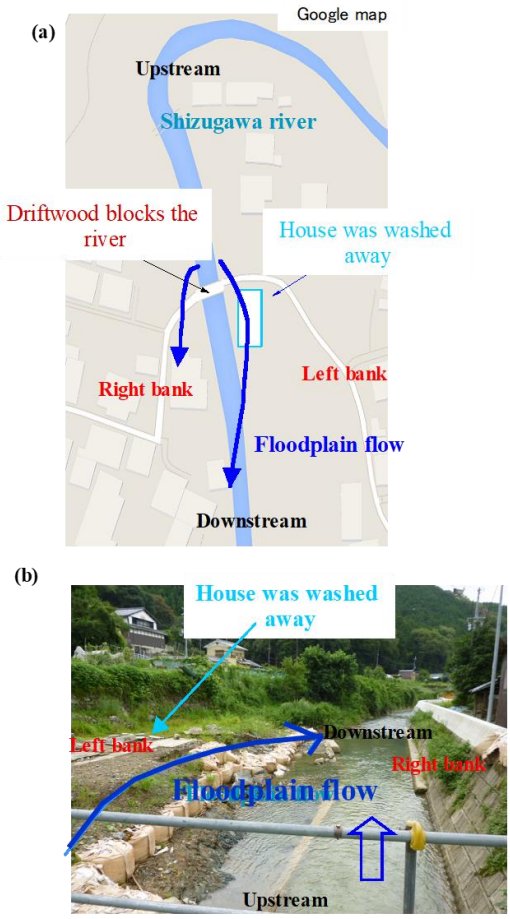

Fig.1 Driftwood blocking and flood damage by floodplain flow (Aug. 2012, Uji Japan)

Many researchers have investigated the woody debris at bridges. Shimizu and Osada 2007 revealed that the branches of driftwood promoted the driftwood accumulation at a bridge using numerical simulation. Schmocker and Hager 2011 conducted flume experiments and evaluated the blocking probability of driftwood (single logs and single root stocks) at bridge decks.

Some previous researchers have investigated the driftwood capturing structure to remove woody debris from the river. To reduce the accumulation probability of driftwood at pier, Lyn et al. 2003 examined the effect of the vertical cylindrical defector upstream of bridge piers. Shalko et al. 2019 investigated the efficiency of a large wood fin and bottom sills upstream of bridge piers.

Schmocker and Weitbrecht 2013 presented a novel driftwood retention structure where the driftwood is retained in a bypass channel located at the outer river bend. Pfister et al. 2013 investigated the blocking probability of driftwood at the piano weir and the upstream water elevation due to driftwood accumulation.

Table1 Hydraulic condition

	Q (l/s)	U_m (m/s)	H (cm)	l (cm)	L_1 (cm)	L_2 (cm)	Re	Fr	Experimental method
Case0	8.0	40.0	10.0	6.0	-	-	40000	0.40	Driftwood capturing experiment,PIV
CaseG1-1	8.0	40.0	10.0	6.0	3.0	-	40000	0.40	Driftwood capturing experiment
CaseG1-2	8.0	40.0	10.0	6.0	3.5	-	40000	0.40	Driftwood capturing experiment
CaseG1-3	8.0	40.0	10.0	6.0	3.8	-	40000	0.40	Driftwood capturing experiment
CaseG1-4	8.0	40.0	10.0	6.0	4.0	-	40000	0.40	Driftwood capturing experiment
CaseG1-5	8.0	40.0	10.0	6.0	4.2	-	40000	0.40	Driftwood capturing experiment
CaseG1-6	8.0	40.0	10.0	6.0	4.5	-	40000	0.40	Driftwood capturing experiment
CaseG1G2	8.0	40.0	10.0	6.0	3.8	3.0	40000	0.40	Driftwood capturing experiment,PIV

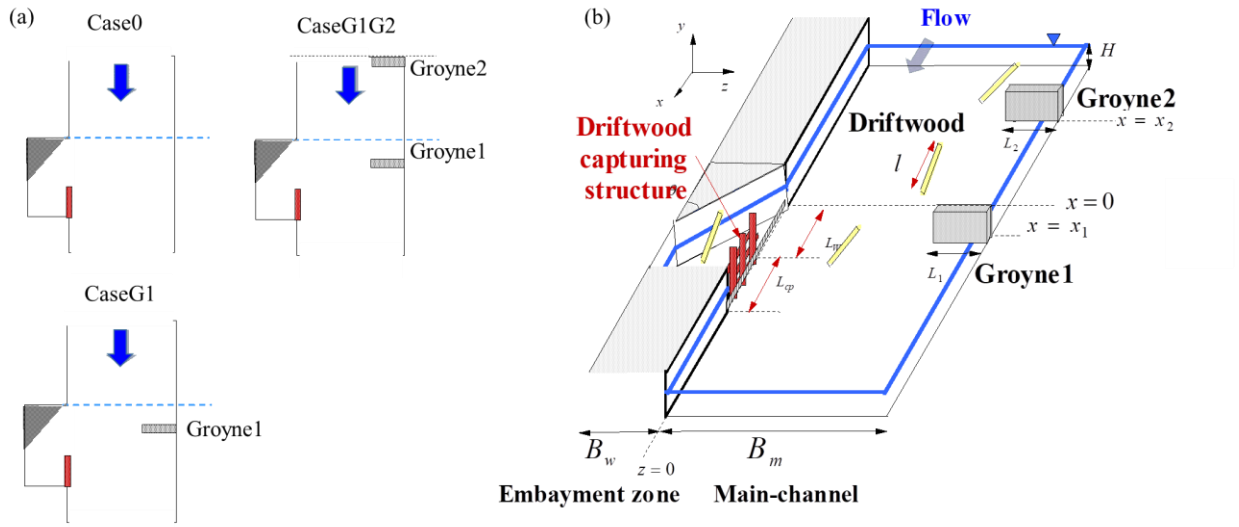

Figure 2 Driftwood capturing structure by embayment zone

In the present study, we considered the driftwood capturing structure by using an embayment zone. Recently, an anti-flood pond (rectangular embayment zone) is used to remove the woody debris in Japan. However, there are few experimental studies published on the removal of driftwood by the embayment zone. The laboratory flume experiments were conducted and we investigated the driftwood trapping probability in the embayment zone.

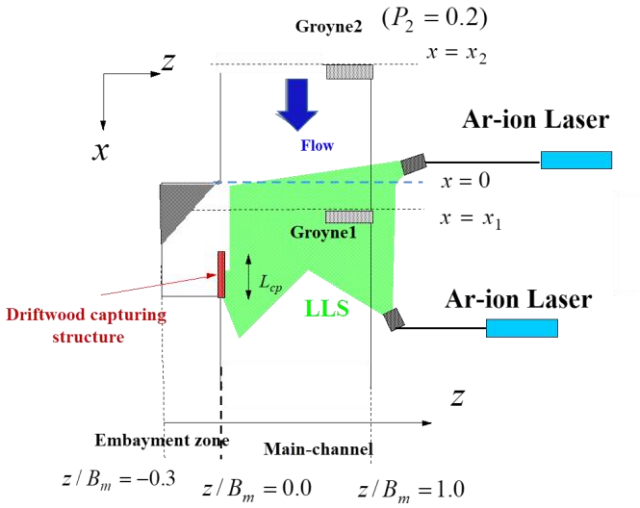

Figure 3 Velocity measurement by PIV

2. METHOD

Figure 2 shows the experimental set-up and the coordinate system. The flume experiments were conducted in a 10m long and 40cm wide glass-made flume. The x-axis is in the streamwise direction, with x=0 at the upstream edge of the embayment zone. The y-axis is in the vertical direction, with y=0 at the channel bed. The z-axis is in the spanwise direction, with z=0 at the pond/mainstream boundary. U, V and W are the time-averaged velocity components in the streamwise, vertical and spanwise velocity components, respectively.

The river bank is modeled by lacing acrylic boxes (length 0.6m, width 0.2m, height 0.25m). One box was removed to create the embayment zone. B_m=20cm is the main-channel width. The embayment zone is 6cm width and 90cm length. The mesh board (1.5× 1.5cm) was used at the pond/mainstream boundary to capture the model logs. The opening length of the embayment zone is L_w=50cm. The entrance shape of the embayment zone is triangle (Fig.2 (a)). From preliminary experiments, the trapping probability is larger for triangle shape than for rectangular shape.

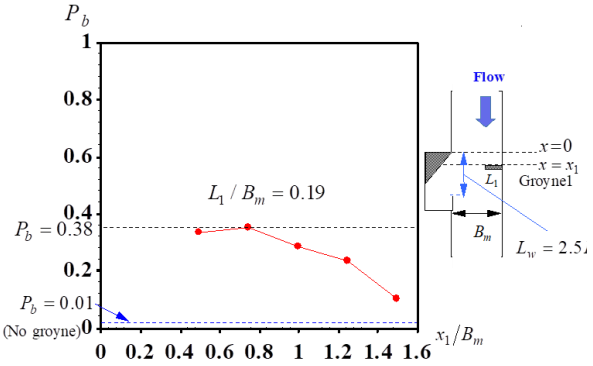

Figure 4 Trapping probability of logs by embayment zone for single groyne case (effect of groyne position)

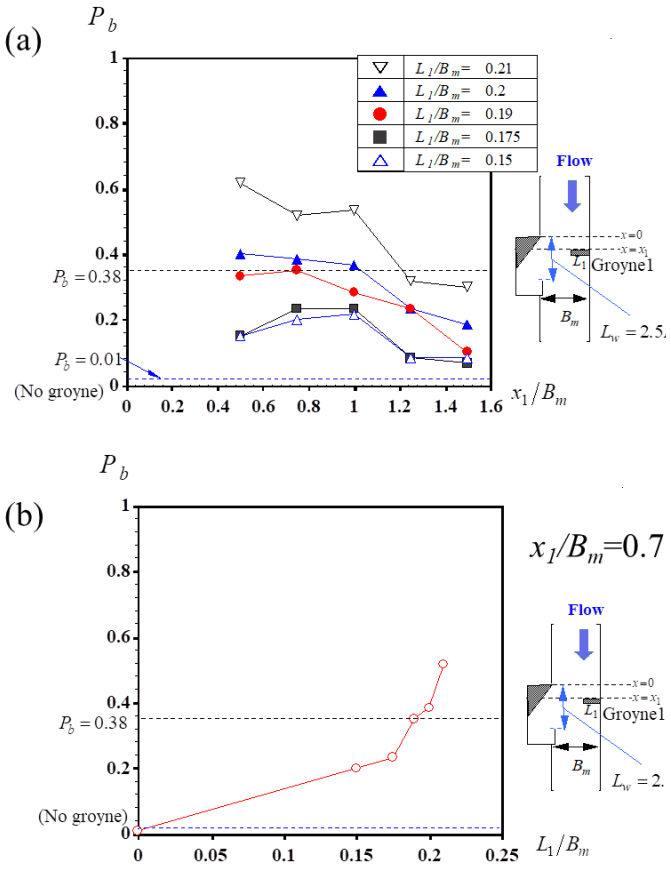

Figure 5 (a) Distribution of trapping probability of logs by embayment zone for single groyne case (effect of groyne position), (b) Effect of groyne length on trapping probability of logs

In the present study, to induce the model logs toward the embayment zone, the groyne is installed on the opposite side of the embayment zone. x_1 and x_2 are the streamwise positions of the Groyne 1 and the Groyne 2, respectively.

Cylinder wood pieces (d=6.0mm diameter and l=6.0cm) were used to model driftwood. The present model logs have no branches. The branches do not affect the followability of the logs because the flow depth is much larger than the diameter of the log. The wood density is 0.6g/cm^3. The wood pieces were soaked in water for 1 hour prior to a test. Model logs were supplied to the flow at 4.0m upstream from the embayment zone (x=-4.0m). Experiments were conducted by adding the group of the model logs continuously to the approach flow over the test duration. The number of supplied wood pieces was 100 pieces. We evaluated the trapping probability of model logs P_b in the embayment zone.

Flow velocity around the embayment zone was measured by particle image velocimetry (PIV: Okamoto and Nezu 2013, Sanjou et al. 2018). In order to obtain two velocity-components, i.e., $\tilde{u}(t)$ and $\tilde{w}(t)$ on x-z horizontal plane (20cm× 20cm), a laser-light sheet (LLS) was projected into the water column horizontally, as shown in Fig.3. The illuminated flow pictures were taken by a high-speed Charge Coupled Device (CCD) camera (1024 ×1024pixels) with 500Hz frame-rate and 60s sampling time. The vertical position of LLS is y/H=0.5. The instantaneous velocity components $(\tilde{u}, \tilde{w})$ on horizontal plane were calculated by the PIV algorithm.

Table1 shows the hydraulic condition. Experiments were conducted on the basis of eight flow scenarios, in which the Groyne length and groyne position were changed. L_1 and L_2 are the lengths of the Groyne 1 and Groyne 2, respectively. The bulk mean velocity is U_m=40.0(cm/s) and the flow depth in Main-channel is H=10cm (see Fig.1).

3. RESULTS

3.1 Effect of groyne length on trapping probability

Figure 4 shows the trapping probability of the log P_b in the embayment zone for Case G1-3. The trapping probability of the log P_b is calculated by:

$$P_b = \frac{n_{tr}}{n_t} \tag{1}$$

n_{tr} is number of trapped logs in embayment zone and n_t is total number of supplied logs. The result of Case 0 (No groyne case) is also indicated. The Groyne 1 length is L_1/B_m=0.19. For Case 0 (No groyne case), the model logs are not trapped in the embayment zone on the right bank side. This implies that the higher velocity occurs on the left bank side and the model logs are concentrated on the left bank side.

In contrast, for Case G1-3 (Groyne1 is installed), the model logs are trapped in the embayment zone. The strong rightward flow (W<0) occurs in front of Groyne 1 and the model logs on the left bank side are induced to the embayment zone. The effect of the groyne position is also observed. The trapping probability of the log

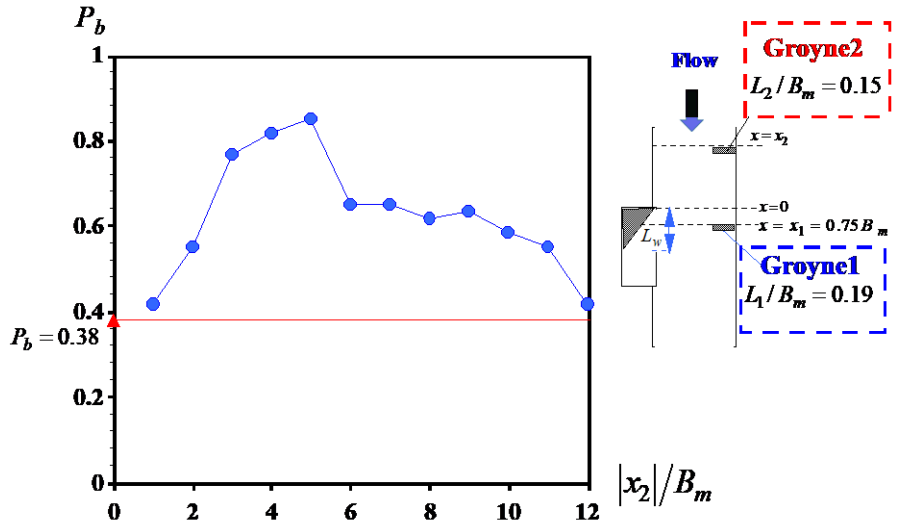

Figure 6 Trapping probability of logs by embayment zone for Case G1G2 (groyne 1 and groyne 2)

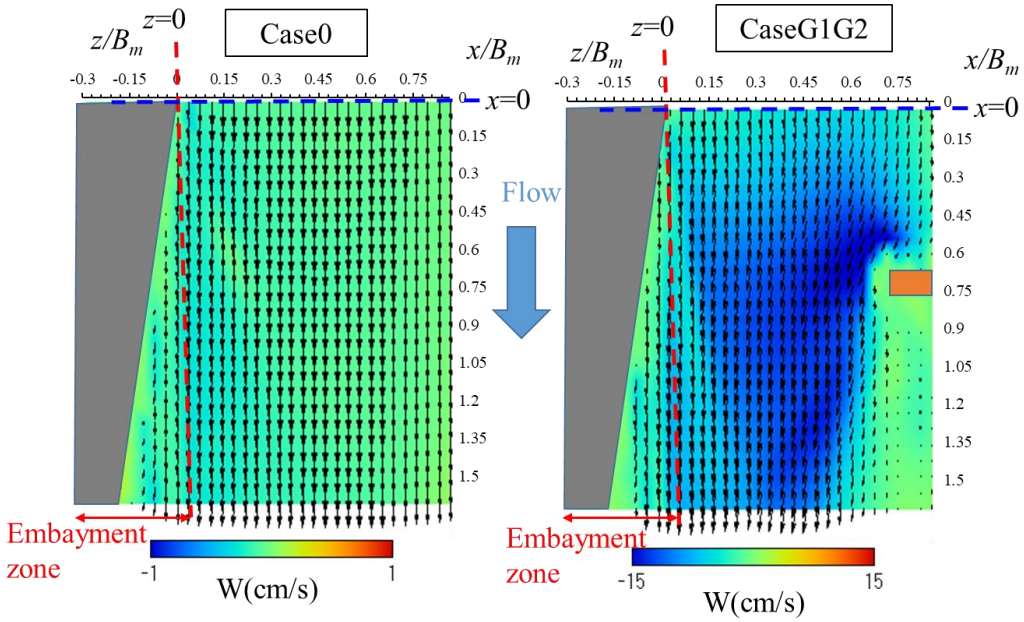

Figure 7 Contours of the time-averaged spanwise velocity *W* on *x*-*z* horizontal plane

P_b becomes largest at x_1/B_m=0.75 (P_b=0.38). This indicates that the rightward flow flows into the embayment zone when the streamwise position of the Groyne 1 is x_1/B_m=0.75.

Figure 5 shows the trapping probability of the model logs P_b in the embayment zone for Case G1-1~6. The groyne1 length is L_1/B_m=0.15, 0.175, 0.19, 0.2 and 0.21. For L_1/B_m=0.21, the maximum value is P_b=0.6 when x_1/B_m=0.5. For L_1/B_m=0.15, the maximum value is P_b=0.2 when x_1/B_m=1.0. These results indicate that the strength and the direction of the rightward flow (W<0) depend on the groyne length. The trapping probability of the model logs increases with an increase of the groyne length L_1.

3.2 Effect of groyne number on trapping probability

By increasing the groyne length, model logs can be removed from the river more efficiently. However, there is a limit to increasing the groyne length. In the present study, Groyne2 was installed upstream of Groyne1. The rightward flow in front of Groyne2 induces model logs to the right bank side upstream of Groyne1 (x<0) and woody debris can be trapped in the embayment zone efficiently without using long groyne.

Figure 6 shows the trapping probability of the model logs P_b in the embayment zone for Case G1G2 (Groyne1 and Groyne2 are installed). Groyne1 length is L_1/B_m=0.19 and the streamwise position of Groyne1 is x_1/B_m=0.75. Groyne2 length is L_2/B_m=0.15. (L_1/B_m<0.2, L_2/B_m<0.2)

The trapping probability of the model logs P_b becomes largest at x_2/B_m=-5.0. These results suggest that when the distance between Groyne1 and Groyne2 ($L_{12}=x_1-x_2$) is close, the flow velocity is reduced behind Groyne1

and consequently, the rightward flow in front of Groyne1 becomes weaker. As the distance between Groyne1 and Groyne2 (L_{12}) increases, the flow velocity in front of Groyne1 increases and the strong rightward flow occurs around Groyne1 (P_b increases).

When the distance L_{12}/B_m exceeds 5.75, the trapping probability of the logs P_b becomes smaller. This implies that the rightward flow in front of Groyne2 reaches the peak value at x_2/B_m=-5.0 and the effect of Groyne2 decreases with an increase of the distance L_{12}/B_m.

Figure 7 shows the contours of the time-averaged spanwise velocity W on x-z horizontal plane. The x-axis and the z-axis are normalized by the main-channel width B_m. Groyne1 length is L_1/B_m=0.19 and the streamwise position of Groyne1 is x_1/B_m=0.75. Groyne2 length is L_2/B_m=0.15 and the streamwise position of Groyne2 is x_2/B_m=-5.0.

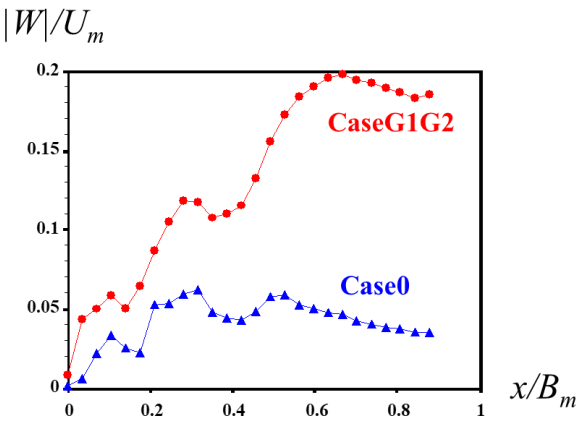

Figure 8 Streamwise distribution of time-averaged spanwise velocity W at the embayment/mainstream boundary (z/B_m=0, red line in Figure 7)

For Case 0 (No groyne case), the weak rightward flow occurs near the embayment/mainstream boundary. The model logs floating near the center of main-channel are not trapped in the embayment zone.

For Case G1G2 (Groyne2 was installed upstream of Groyne1), the strong rightward flow occurs upstream of the Groyne 1. The model logs floating near the center of main-channel are induced to the right bank side.

Figure 8 shows the streamwise distribution of time-averaged spanwise velocity $|W|$ (x) at the embayment/mainstream boundary (z/B_m=0, red line in Figure 7). For Case 0 (No groyne case), the values of the spanwise velocity are small. For Case G1G2, the spanwise velocity increases in the streamwise direction and takes the maximum value at x/B_m=0.7.

The present results revealed that the model logs are not trapped in the embayment zone without groynes. The groyne on the opposite side of the embayment zone induces the model logs toward the embayment zone. The trapping probability is influenced by the groyne position, length and numbers. In the future, we will investigate the effect of porosity of groyne and installation angle.

4. CONCLUSIONS

In the present study, we considered the driftwood capturing structure using an embayment zone. The laboratory flume experiments were conducted and we investigated the driftwood trapping probability in the embayment zone.

Main findings are as follows:

1. For Case 0 (No groyne case), the model logs are not trapped in the embayment zone on the right bank side. For Case G1-3 (Groyne1 is installed), the strong rightward flow (W<0) occurs in front of Groyne 1 and the model logs on the left bank side are induced to the embayment zone. The effect of the groyne position is also observed. The trapping probability of the model logs P_b becomes largest at x_1/B_m=0.75 (P_b=0.38).

2. For Case G1G2 (Groyne2 was installed upstream of Groyne1), woody debris can be trapped in the embayment zone efficiently without using long groyne. The trapping probability of the model logs P_b becomes largest at x_2/B_m=-5.0 (P_b=0.85).

3. For Case 0 (No groyne case), the weak rightward flow occurs near the embayment/mainstream boundary. The model logs floating near the center of main-channel are not trapped in the embayment zone. For Case G1G2 (Groyne2 was installed upstream of Groyne1), the strong rightward flow occurs upstream of the Groyne 1. The model logs floating near the center of main-channel are induced to the right bank side.

ACKNOWLEDGMENTS

The present study was carried out under the financial support of the Research Project Grant-In-Aid for Scientific Research of Japanese Government (Kakenhi No.18K13968, Principle Investigator= T. Okamoto). The authors gratefully acknowledge this support.

REFERENCES

Lyn D.A., Cooper T., Yi Y.K., Sinha R., & Rao A.R. (2003). Debris accumulation at bridge crossings: Laboratory and field studies. Paper presented at Joint Transportation Research Program, Report No.: FHWA/IN/JTRP-2003/10, Purdue University, West Lafayette, IN, USA.

Okamoto, T., Takebayashi, H., Kaneko, T., Shibayama, Y. and Toda, K. (2016): Flood-flow characteristics in a blocked river: Detour flow around a bridge, *Proc. of Riverflow2016 Congress, St. Louis*, pp.1869-1876

Okamoto, T., and Nezu, I. (2013). Spatial evolution of coherent motions in finite-length vegetation patch flow. Environmental Fluid Mechanics, 13(5), 417–434

Pfister, M., Capobianco, D., Tullis, B. & Scheiss, A. (2013) Debris-Blocking Sensitivity of Piano Key Weirs under Reservoir-Type Approach Flow. *J. Hydraul. Eng.*, 139, pp.1134-1141.

Sanjou, M., Okamoto, T., and Nezu, I. (2018): Dissolved oxygen transfer into a square embayment connected to an open-channel flow, *International Journal of Heat and Mass Transfer*, 125, pp. 1169-1180.

Schalko I., Schmocker L., Weitbrecht, V. and Boes, R.M. (2019). Risk reduction measures of large wood accumulations at bridges, *Environmental Fluid Mechanics*, https://link.springer.com/article/10.1007%2Fs10652-019-09719-4

Schmocker, L., and Hager, W.H (2011): Probability of drift blockage at bridge decks, *J. Hydraul. Eng.*, Vol.137, pp.470-479.

Schmocker, L. and Weitbrecht, V. (2013): Driftwood: Risk Analysis and Engineering Measures, *J. Hydraul. Eng.*, 139(7), pp.683-695

Shimizu, Y. and Osada, K.: Numerical experiments on accumulation process of driftwoods around piers by using a DEM-FLOW coupling model. *Annual J. Hydraul. Eng. JSCE*, 51, pp.829– 834, 2007. (Japanese)